ARTICLE TYPE

A stable graphite negative electrode for the lithium-sulfur battery

Fabian Jeschull,[a] Daniel Brandell[a], Kristina Edström,[a] and Matthew J. Lacey[a]
Post-print accepted by *Chem Commun*. Now published at doi: 10.1039/C5CC06666B

Efficient, reversible lithium intercalation into graphite in ether-based electrolytes is enabled through a protective electrode binder, polyacrylic acid sodium salt (PAA-Na). In turn, this enables the creation of a stable "lithium-ion-sulfur" cell, using a lithiated graphite negative electrode with a sulfur positive electrode, using the common DME:DOL solvent system suited to the electrochemistry of the lithium-sulfur battery. Graphite-sulfur lithium-ion cells show average coulombic efficiencies of ∼99.5%, compared with <95% for lithium-sulfur cells, and significantly better capacity retention, taking into account cell balancing considerations. The high efficiency derives from the considerably better interfacial stability of the graphite electrode, which suppresses the polysulfide redox shuttle and self-discharge.

The lithium-sulfur (Li-S) battery is an attractive energy storage system for transport applications, e.g., electrical vehicles, because of its high gravimetric energy density[1]. However, the often high solubility of the polysulfide intermediates of the cell reaction give rise to a self-discharge mechanism, known as the polysulfide redox shuttle[2]. With the recent resurgence of interest in this system, many new approaches to mitigating the shuttle reaction have been proposed. Notable examples include the electrolyte additive $LiNO_3$[3–5], restriction of polysulfide mass transport by interlayers or selective separators[6–8], active adsorption of polysulfides by functional binders[9] or metal oxides[10,11], and non-solvents for polysulfides[12–14].

Despite these recent advances, there has been relatively little progress in the development of the negative electrode for this system. Well-documented severe morphological changes at the

lithium metal electrode on cycling[15,16] continue to present a serious challenge, even after three decades of active lithium-metal battery research. A constantly changing lithium surface generates new surface area upon repeated cycling, resulting in continuous and irreversible electrolyte decomposition, continuous growth of the solid-electrolyte interphase (SEI), loss of lithium inventory and electrical contact of lithium domains, and ultimately rapid cell failure.

Most current academic research focuses on the positive (sulfur) electrode, with the electrolyte and Li electrode used in vast excess. The inefficiency of the negative electrode and associated electrolyte degradation are, subsequently, rarely observed. In fact, electrolyte volumes and Li electrode thicknesses are often not even reported in most published work. Reduced electrolyte and Li electrode excesses typically lead to significant capacity fade and/or cell failure within the first hundred cycles, even at moderate sulfur loadings and independent of the optimisation of the positive electrode.

For these reasons, alternative negative electrode materials for the Li-S system have been investigated. Materials which alloy with lithium, such as tin[17,18] and silicon[19–21], are attractive in terms of energy density. The development of the silicon electrode for lithium-ion (Li-ion) batteries, in particular, has been such that stable, reversible cycling over thousands of cycles can be demonstrated, if the degree of lithiation is suitably controlled. However, the relatively large volume expansion of these materials on lithiation, leading to electrode disintegration and continuous growth of the SEI, remain concerns.

Graphite has been the mainstay negative electrode of the Li-ion battery since its inception. Despite a comparatively low theoretical capacity of 372 mAh g^{-1}, the relatively small volume expansion of graphite on intercalation and a stable SEI enable good stability. To the best of our knowledge, only two articles report the use of graphite as the negative electrode in a Li-S battery[22,23]. In both of these cases, an electrolyte based on carbonate solvents was used, as is overwhelmingly the standard for

Li-ion batteries. However, it is now well-established that carbonate solvents are, in most cases, unsuitable for the lithium-sulfur system, since sulfur utilisation at even moderate sulfur contents is very poor, and the solvents are susceptible to irreversible reactions with polysulfides[24]. Electrolytes based on ether solvents are now the most commonly-used electrolytes for the lithium-sulfur system, although said electrolytes have long been considered as unsuitable for graphite electrodes, due to the breakdown of both electrolyte and electrode caused by solvent intercalation[25]. Other carbon materials, such as hard carbon, are not as susceptible to this issue, and their direct compatibility with ether-based electrolytes and relatively good cycle life in Li-S cells has been demonstrated elsewhere[26].

Recent studies have shown however that even in "aggressive" electrolyte environments, graphite exfoliation can be prevented by careful choice of the binder, which can act as a protecting layer at the electrode-electrolyte interface[27–30]. In a comparative study, our group has demonstrated that the interfacial stability of graphite particles is closely linked to the surface coverage and the "swellability" of the binder in the electrolyte[31]. The sodium salts of carboxymethyl cellulose (CMC-Na) and polyacrylic acid (PAA-Na) enable greatly improved cycling stability and higher coulombic efficiencies in electrolytes based on propylene carbonate (PC) in comparison to the standard poly(vinylidene difluoride) (PVdF)-based binders.

This improved interfacial and cycling stability similarly extends to other electrolyte systems. In this work, we demonstrate for the first time the stable cycling of a graphite electrode in an ether-based electrolyte, and a full, balanced "Li-ion-sulfur" cell using a lithiated graphite as the lithium source. The stable cycling is enabled through the protective effect of PAA-Na used as the binder. While it is still a matter of debate as to whether such a graphite-sulfur system can deliver a high enough energy density to be a viable alternative to the Li-ion system, the investigation of this system nonetheless provides important insights into the behaviour of the negative electrode in the sulfur-based battery system.

Following on from our previous study[31] we assessed the cycling stability of graphite electrodes in a standard electrolyte for Li-S (1 M LiTFSI, 0.25 M LiNO$_3$ in 1:1 1,2-dimethoxyethane:1,3-dioxolane (DME:DOL)) with various binders: a PVdF copolymer (poly(vinylidene difluoride-co-hexafluoropropylene), PVdF-HFP), CMC-Na and PAA-Na. As with our previous work, PAA-Na was found to give the highest discharge capacities, close to the theoretical capacity of graphite. The inclusion of LiNO$_3$ in the electrolyte was however found to be required for stable cycling, indicating its importance in SEI formation (see Supporting Information, Figure S1). Without LiNO$_3$, the electrode and electrolyte showed signs of severe decomposition, regardless of binder, within a few cycles. Graphite electrodes with a PAA-Na binder and LiNO$_3$ showed the typical reversible and staged voltage profile characteristic of lithium intercalation into graphite. A comparison of the voltage profiles of electrodes with PAA-Na, CMC-Na or PVdF-HFP, with and without LiNO$_3$ in the electrolyte, is given in the Supporting Information, Figure S1. The stable cycling performance of a graphite electrode with a PAA-Na binder and LiNO$_3$ electrolyte additive over 50 cycles is presented in Fig-
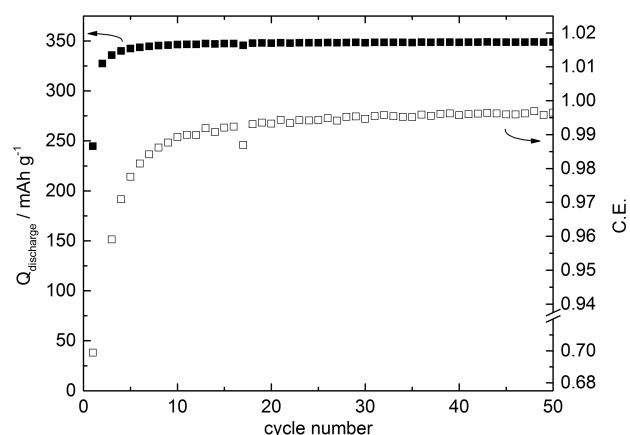
Fig. 1 Galvanostatic cycling of a graphite electrode containing PAA-Na binder in the LiTFSI/LiNO$_3$/DME:DOL electrolyte system at C/10 rate.

ure 1. The full comparison of the binders and electrolyte formulations is given along with a complete experimental procedure in the Supporting Information.

All sulfur-based cells were prepared in CR2025-format coin cells. Lithium-sulfur cells were compared as references for the graphite-sulfur cells. Lithium foil electrodes of different thicknesses (125 μm, "thick", and 30 μm, "thin", corresponding to ~2000% and ~500% excesses of Li relative to the positive electrode respectively) were used. Graphite electrodes for graphite-sulfur cells were first prepared in pouch cells by cycling against Li in the LiTFSI/LiNO$_3$/DME:DOL electrolyte several times. The electrodes were extracted in the fully lithiated state, washed with a mixture of DME and DOL, and assembled into coin cells against sulfur positive electrodes. The positive electrodes (58% w/w S$_8$ in the electrode) were prepared from a simple sulfur-carbon composite electrode with a water-based binder of carboxymethylcellulose and styrene-butadiene rubber (CMC:SBR) similar to those used in our previous work[32]. These electrodes typically deliver maximum reversible capacities in the range 1000-1100 mAh g$_S^{-1}$. The electrolyte volume was reduced to the minimum value at which stable cycling was still observable (6 μL mg$_S^{-1}$). Graphite-sulfur cells were assembled with a target theoretical excess of 20 – 30% of sulfur, relative to the capacity of the negative electrode. Taking into account the lower practical capacities of the positive electrode, this translates to a 15 – 40% excess of Li at the negative electrode, i.e., considerably lower than with the Li metal electrodes used in this work. A comparison of the discharge capacities and coulombic efficiencies of these cells is presented in Figure 2. For comparison, the 125 μm-thick lithium electrode used as the counter-electrode in the pre-cycling of the graphite electrode was also extracted and assembled into a Li-S cell and is noted here as "cycled Li". Coulombic efficiency is defined here as the ratio of the discharge capacity to the charge capacity, that is, efficiencies less than 1 indicate overcharging.

The graphite-sulfur cell shows initial reversible capacities of ~1000 mAh g$_S^{-1}$, which fade roughly linearly to ~800 mAh g$_S^{-1}$ after around 120 cycles. The Li-S cell with the excess "thick"
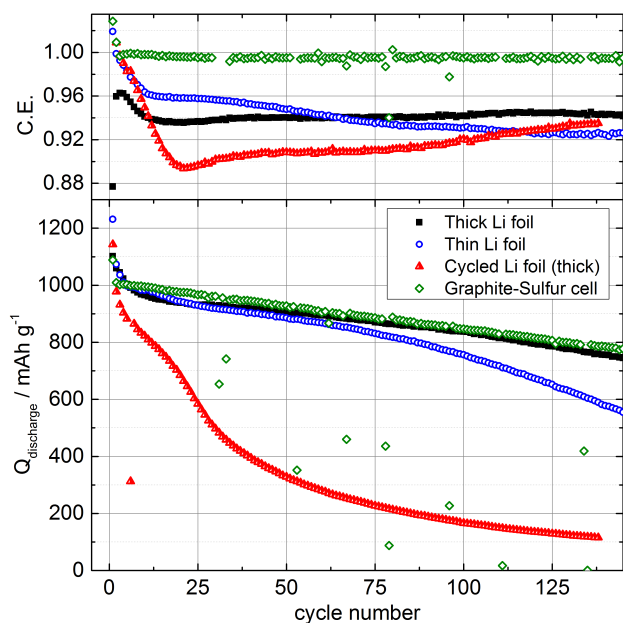
Fig. 2 Discharge capacity and coulombic efficiency vs cycle number for a graphite-sulfur cell compared with three lithium-sulfur cells with different negative electrodes ("thick" Li, "thin" Li, and "cycled" Li) cycled at a constant rate of C/10.

Li electrode exhibits almost the same capacity. However, the graphite-sulfur cell shows a high average coulombic efficiency of >99.5%, compared with values of <95% for all of the Li electrode cases. The graphite electrode for this cell was pre-cycled against lithium for nine cycles. The coulombic efficiency of the graphite-sulfur cell was found to be higher if the graphite electrode was pre-cycled longer in the electrolyte, indicating the importance of developing a sufficiently thick and stable SEI. A comparison with a cell having been pre-cycled for six cycles is given in the Supporting Information. The high coulombic efficiency reflects a reduced effect of the polysulfide redox shuttle; we shall return to this point later.

Cells with "cycled Li" electrodes showed, before assembly into the Li-S cell, the expected black and rough morphology consistent with the inefficient stripping/plating reactions of Li metal. Surprisingly, when used as the negative electrode with fresh electrolyte and a fresh sulfur positive electrode, the cell showed unusually rapid capacity fade. This observation clearly demonstrates the importance of compounds derived from polysulfides on the morphology and stability of the SEI on the Li electrode, consistent with recent observations made elsewhere[33]. The synergetic influence of polysulfides and $LiNO_3$ on the morphology and efficiency of Li metal cycling has also very recently been demonstrated elsewhere[34]. Closer investigation of this effect on the behaviour of Li-S cells would be an interesting direction for future work.

It is also clear from Fig. 2 that the cycle life of Li-S cells becomes increasingly dependent on the availability of lithium and the thickness of the foil. After only 90 cycles, there is a clear in-

crease in the rate of capacity fade for the cell with the thin Li negative electrode, despite still being in relatively large excess. The "thick Li" cell shows a roughly linear decrease in capacity over 150 cycles, despite the >2000% excess of Li. This decrease indicates that the capacity fade is more likely due to a decreasing utilisation of sulfur at the positive electrode. That the graphite-sulfur cell shows the same rate of capacity decay also indicates that the graphite electrode is not the limiting electrode in the cell over 150 cycles despite the considerably more restricted Li excess. The influence of the excess of Li metal on the Li surface morphology and, in turn, the cycle life of Li-S cells has previously been reported by Sion Power Corporation[15], and the improved efficiency of graphite, relative to Li metal negative electrodes, when cycled against $LiNi_{1/3}Mn_{1/3}Co_{1/3}O_2$ (NMC) positive electrodes has also been demonstrated.[35] The results here are further evidence of the importance of the negative electrode in the cycle life of Li-S cells even at relatively low positive electrode loadings. The improved stability of the graphite electrodes relative to Li metal can also be seen when estimating changes in cell internal resistance, which is presented in the Supporting Information, Figure S3.

As previously mentioned, a higher coulombic efficiency for the graphite-sulfur cell reflects a decreased overcharge, which strongly indicates a reduction in the rate of the polysulfide shuttle. The reduced shuttle effect, in turn, results in a reduced rate of self-discharge, since polysulfides remaining in the electrolyte continue to be reduced by the negative electrode and subsequently drive the dissolution of sulfur from the positive electrode. To quantify this, we cycled a Li-S cell with a thick Li negative electrode and a graphite-sulfur cell at C/10 but allowed the cell to rest at OCV following a complete charge every three cycles. The rest time was varied from 12 hours to as long as 14 days. The voltage profile and drop in capacity during the resting time allows for the determination of the extent of self-discharge. A comparison of the graphite-sulfur and Li-S cells is given in Figure 3.

Both cells again show similar initial capacities over the first few cycles. Both cells also show losses in capacity after long rest periods, especially for rest periods of three or more days. However, the graphite-sulfur cell shows clearly better retention of capacity, both during extended rest periods and over a larger number of cycles (i.e., the self-discharge is largely reversible). It is easily seen that the sulfur-graphite cell retains its upper voltage plateau at ~2.25 V considerably better than the Li-S cell, which shows the transition to the lower voltage plateau within only three days. Note the decreased voltage of the graphite cell with respect to the Li-S cell due to the slightly higher potential of the graphite electrode. The graphite-sulfur cell, on the other hand, retains its upper plateau for approximately ten days. By comparing the reversible capacity losses of the two cells over a rest period of 3 days, we estimate that the rate of self-discharge for the graphite-sulfur cell within this time is roughly one-fifth of that of the Li-S cell.

In summary, shelf-life and self-discharge rate are important properties for most of the potential applications of the Li-S system but have unfortunately received relatively little attention from the academic field. While $LiNO_3$ is effective in reducing the polysulfide redox shuttle, to the extent that cells can be cycled with po-
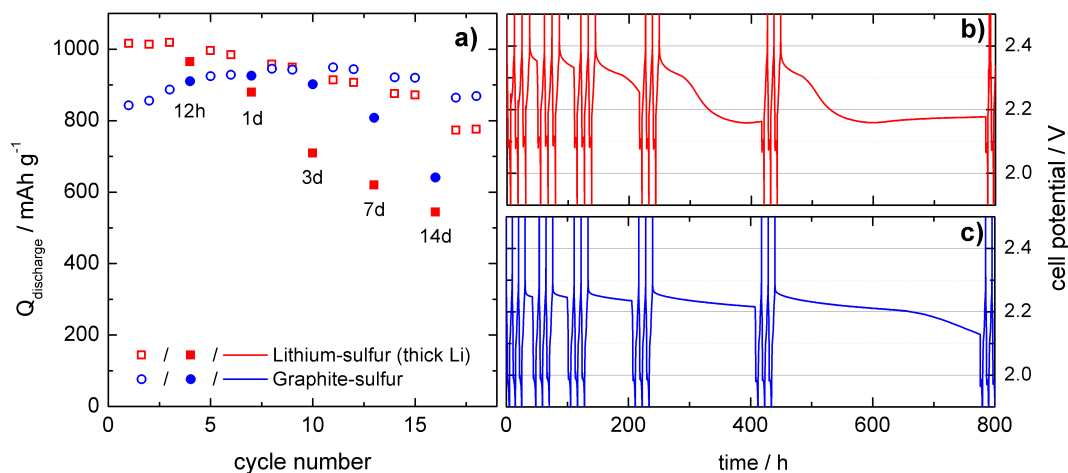
Fig. 3 Comparison of self-discharge behaviour of a lithium-sulfur cell with a lithiated graphite-sulfur cell. a) discharge capacities vs cycle number, where a filled point represents the discharge capacity after an OCV rest period following end of the previous cycle. The OCV time is indicated below the filled data point. b, c) Voltage profiles for the cells over the duration of this experiment.

tential limitation alone at slow rates, the shuttle effect nonetheless remains and, as is clearly demonstrated here, causes significant capacity loss over periods of only a few days. Furthermore, LiNO$_3$ is known to be gradually consumed at the electrode, which can result in an increasing rate of self-discharge after prolonged usage.

Average coulombic efficiencies of 99.5% and considerably reduced self-discharge demonstrate that improving the interfacial stability of the anode can be, as well as optimising the electrolyte and positive electrode, a valuable approach to improving the lifetime and commercial viability of this system. The improved stability is most likely a result of the considerably more stable graphite-electrolyte interface compared with the Li-electrolyte interface; no fresh graphite surface needs to be exposed during cycling and a relatively small volume change of the material ensures that the SEI is not compromised to a significant extent. Compositional differences in the SEI have not been investigated here, but this would be a valuable direction for future research.

The stability of the lithium negative electrode is a frequently overlooked bottleneck in the development of this system. Although graphite may not be practically viable for high-energy sulfur cells, we believe that this work demonstrates that continued efforts to improve the efficiency of lithium cycling, and the development of alternatives, such as high-energy silicon electrodes, remain of key importance. This approach is furthermore entirely complementary and compatible with the existing developments being made with the positive electrode and electrolyte.

Acknowledgements

References

1 P. G. Bruce, S. A. Freunberger, L. J. Hardwick and J. M. Tarascon, *Nat. Mater.*, 2012, **11**, 19–29.
2 Y. V. Mikhaylik and J. R. Akridge, *J. Electrochem. Soc.*, 2004, **151**, A1969–A1976.
3 Y. V. Mikhaylik and (Sion Power Corporation), *Methods of charging lithium sulfur cells. U.S. Patent 7646171*, 2008.
4 S. S. Zhang, *J. Electrochem. Soc.*, 2012, **159**, A920–A923.
5 S. S. Zhang, *Electrochim. Acta*, 2012, **70**, 344–348.
6 X. Wang, Z. Wang and L. Chen, *J. Power Sources*, 2013, **242**, 65–69.
7 Y. S. Su and A. Manthiram, *Nat. Commun.*, 2012, **3**, 1166.
8 I. Bauer, S. Thieme, J. Brückner, H. Althues and S. Kaskel, *J. Power Sources*, 2014, **251**, 417–422.
9 M. J. Lacey, F. Jeschull, K. Edström and D. Brandell, *J. Power Sources*, 2014, **264**, 8–14.
10 X. Liang, C. Hart, Q. Pang, A. Garsuch, T. Weiss and Linda F. Nazar, *Nat. Commun.*, 2015, **6**, 5682.
11 Q. Pang, D. Kundu, M. Cuisinier and L. F. Nazar, *Nat. Commun.*, 2014, **5**, 1–19.
12 K. Ueno, J. W. Park, A. Yamazaki, T. Mandai, N. Tachikawa, K. Dokko and M. Watanabe, *J. Phys. Chem. C*, 2013, **117**, 20509–20516.
13 L. Suo, Y.-S. Hu, H. Li, M. Armand and L. Chen, *Nat. Commun.*, 2013, **4**, 1481.
14 M. Cuisinier, P.-E. Cabelguen, B. D. Adams, A. Garsuch, M. Balasubramanian and L. F. Nazar, *Energy Environ. Sci.*, 2014, **7**, 2697.
15 Y. V. Mikhaylik, I. Kovalev, R. Schock, K. Kumaresan, J. Xu and J. Affinito, ECS Trans., 2010, pp. 23–34.
16 R. Bhattacharyya, B. Key, H. Chen, A. S. Best, A. F. Hollenkamp and C. P. Grey, *Nat. Mater.*, 2010, **9**, 504–510.
17 J. Hassoun and B. Scrosati, *Angew. Chem. Int. Ed.*, 2010, **49**, 2371–2374.
18 J. Hassoun, Y. K. Sun and B. Scrosati, *J. Power Sources*, 2011, **196**, 343–348.
19 R. Elazari, G. Salitra, G. Gershinsky, A. Garsuch, A. Panchenko and D. Aurbach, *Electrochem. commun.*, 2012, **14**, 21–24.
20 Y. Yang, M. T. McDowell, A. Jackson, J. J. Cha, S. S. Hong and Y. Cui, *Nano Lett.*, 2010, **10**, 1486–1491.
21 J. Brückner, S. Thieme, F. Böttger-Hiller, I. Bauer, H. T. Grossmann, P. Strubel, H. Althues, S. Spange and S. Kaskel, *Adv. Func. Mater.*, 2014, **24**, 1284–1289.
22 S. Zheng, Y. Chen, Y. Xu, F. Yi, Y. Zhu, Y. Liu and J. Yang, *ACS Nano*, 2013, **7**, 10995–11003.
23 X. He, J. Ren, L. Wang, W. Pu, C. Wan and C. Jiang, *ECS Trans.*, 2007, **2**, 47–49.
24 S. Zhang, K. Ueno, K. Dokko and M. Watanabe, *Adv. Energy Mater.*, 2015, 1500117.
25 D. Aurbach, a. Zaban, Y. Ein-Eli, I. Weissman, O. Chusid, B. Markovsky, M. Levi, E. Levi, a. Schechter and E. Granot, *J. Power Sources*, 1997, **68**, 91–98.
26 S. Thieme, J. Brückner, A. Meier, I. Bauer, K. Gruber, J. Kaspar, A. Helmer, H. Althues, M. Schmuck and S. Kaskel, *J. Mater. Chem. A*, 2015, **3**, 3808–3820.
27 S. Komaba, T. Ozeki and K. Okushi, *J. Power Sources*, 2009, **189**, 197–203.
28 S. Komaba, N. Yabuuchi, T. Ozeki, K. Okushi, H. Yui, K. Konno, Y. Katayama and T. Miura, *J. Power Sources*, 2010, **195**, 6069–6074.
29 J.-H. Lee, S. Lee, U. Paik and Y.-M. Choi, *J. Power Sources*, 2005, **147**, 249–255.
30 H. Buqa, M. Holzapfel, F. Krumeich, C. Veit and P. Novák, *J. Power Sources*, 2006, **161**, 617–622.
31 F. Jeschull, M. J. Lacey and D. Brandell, *Electrochim. Acta*, 2015, in press.
32 M. J. Lacey, K. Edström and D. Brandell, *Electrochem. Commun.*, 2014, **46**, 91–93.
33 W. Li, H. Yao, K. Yan, G. Zheng, Z. Liang, Y.-M. Chiang and Y. Cui, *Nat. Commun.*, 2015, **6**, 7436.
34 W. Li, H. Yao, K. Yan, G. Zheng, Z. Liang, Y.-M. Chiang and Y. Cui, *Nat. Commun.*, 2015, **6**, 7436.

35 R. Younesi, G. M. Veith, P. Johansson, K. Edström and T. Vegge, *Energy Environ. Sci.*, 2015, **8**, 1905–1922.